

TICRA



Study on Advanced Multiple-Beam Radiometers

ESTEC Contract No. 4000107369/12/NL/MH

Executive Summary Report

Provided by: *TICRA, Denmark*

Revision 1.0

September, 2014

S-1580-D3

Issue	Date	Record of changes	Author
1.0	04/09/2014	Initial revision.	Knud Pontoppidan

TABLE OF CONTENTS

1. Introduction	1
2. Radiometer requirements and associated antenna requirements	1
3. Conical scan or push-broom concept	2
4. Feed array design principles	2
5. Push-broom torus reflector antenna	3
5.1 Reflector geometry	3
5.2 RF performance results	4
5.2.1 Central beam at Ku-band	4
5.2.2 Reduction of feed array rows along ϕ	5
5.2.3 Total feed arrays for C-, X- and Ku-band	6
5.2.4 Additional performance checks	7
6. Calibration and RFI mitigation	7
7. Feeding network and receiver issues	8
7.1 Existing state-of-the-art components	8
7.2 Realistic components within a 5 years time frame	8
8. Mechanical design of the push-broom torus antenna	8
9. Summary of results achieved	9
10. Future work	9

1. Introduction

The present Executive Summary Report describes the work performed under the contract 4000107369/12/NL/MH, “Study on Advanced Multiple-Beam Radiometers”. The work has been carried out with TICRA as the main contractor and

DTU-Space, Lyngby, Denmark
Chalmers, Gothenburg, Sweden
HPS, Munich, Germany

as subcontractors.

The oceanographic community has strong interest in high spatial resolution. Current microwave radiometers in space operating at C-band (6.9 GHz) or at higher frequency provide a resolution of around 50 km, whereas less than 20 km is desirable. Current capabilities provide measurements not closer than around 100 km from the shore-line, because of the signal contamination by antenna side-lobes illuminating the land. There is a strong desire to reduce this distance to 5-15 km.

It was the purpose of the present study to design a radiometer which is able to meet these requirements. Two basically different concepts were investigated, a conical scanning antenna and a push-broom antenna, and the most promising concept was selected for further detailed design activities.

This summary is compiled by TICRA, but it includes contributions from all the partners.

2. Radiometer requirements and associated antenna requirements

The instrument requirements as stated in the SOW are shown in Table 1 below. The instrument shall operate in three bands, C-band (6.9 GHz), X-band (10.65 GHz) and Ku-band (18.7 GHz). The

[B] requirements have guided this study. The required 20 km footprint at C-band leads to a large antenna aperture of around 5 m in diameter. This is considerably larger than any radiometer system antenna flown hitherto.

Centre Frequency [GHz]	Bandwidth [MHz]	Polarization	NeAT [K]		Footprint at 3dB [km]
			T	B	
6.9	300	V, H	0.35	0.25	50[T], 20[B], 5[O]
10.65 [Optional]	100	V, H	0.25	0.25	50[T], 20[B], 5[O]
		S ₃ , S ₄	0.25	0.25	
18.7	200	V, H	0.3	0.25	25[T], 10[B], 5[O]
		S ₃ , S ₄	0.3	0.25	

Table 1 List of performance requirements for SST/OVW radiometer.

The radiometer instrument requirements may be used to determine the requirements for the radiometer antenna. One requirement concerns the cross polarisation of the antenna. The radiometer shall measure brightness temperatures in two linear polarisations, vertical and horizontal, and with accuracy within 0.25K. It has been demonstrated that this will be fulfilled when the cross-polar power radiated towards the Earth does not exceed 0.33% of the total power on the Earth.

Another requirement, not shown in Table 1, is extremely interesting and important for the user of radiometric data: the instrument must be able to measure as close as 5-15 km from the coast. This means that the power in the pattern over the land shall be sufficiently small. It has been found that the required accuracy is obtained when the coast line is located outside a cone around the main beam containing 99.72% of the total power on the Earth. In order to obtain a small distance to coast it is therefore of interest to reduce this cone.

The required swath width was set to 1500 km in the SOW. However, it was realised very early in

the study that, as far as push-broom systems are concerned, this is a very demanding requirement which will lead to a very large antenna. It was therefore decided to reduce the swath width to 600 km. Even with this reduction the radiometer will represent a major advancement in the study of the oceans.

3. Conical scan or push-broom concept

It was required from the beginning that the study should include at least one conical scanning antenna and one push-broom antenna. The difference between these two concepts is best understood in connection with Figure 1.

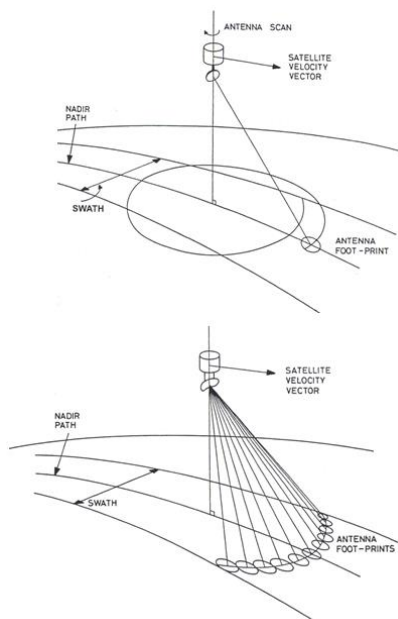


Figure 1 Conical scan (on top) and push-broom (bottom) scenario.

The conical scanning antenna rotates around a vertical axis, and the coverage of the Earth is obtained partly by the movement of the satellite and partly by the rotation. It is easily derived that a radiometer cannot achieve the desired sensitivity in a traditional single radiometer channel/beam concept. The required sensitivity can only be met by considering several

simultaneous beams in a multi-beam scanning system.

For the push-broom system there are no moving parts but the antenna radiates as many beams as required to cover the swath. The push-broom system achieves very high sensitivity since all across track footprints are measured simultaneously by their own receivers. The antenna has the clear advantage of being stationary, but the number of beams and receivers is very high.

4. Feed array design principles

It was realised early in the project that a traditional one beam-per-feed arrangement is not possible and a dense focal plane array will be needed. This means that many array elements take part in the formation of one beam and the same array element takes part in the formation of many beams. The composite feed array must be excited by a multi-mode beam-forming network.

The feed array design was investigated almost independently by both TICRA and Chalmers. To simplify matters the array elements are half-wave dipoles located a quarter of a wavelength above an infinite ground plane. The element only radiates in the upper half space above the ground plane. It is assumed that the elements are arranged in a square lattice. An initial investigation showed that the optimum distance between the array elements is 0.75 wavelength.

Initially TICRA used the Conjugate Field Matching method to determine the feed element excitations. It turned out, however, that this approach is too restrictive and an alternative optimisation method was used which directly optimises the distance to coast. It turns out that the optimisation can be formulated as an eigenvalue problem, where the eigenvalue represents the maximum radiated power inside a

given cone and the eigenvector holds the excitations to generate this field.

The optimisation methods used by TICRA and Chalmers are similar and the difference lies in the way the cost function is defined: it is the ratio of powers inside and outside the angular cone for the case of TICRA; while it is the ratio of power inside a specified small region to noise power outside this region for the case of CHALMERS. It turns out that the performance results obtained for the radiometer are not identical, but similar and good for both procedures.

5. Push-broom torus reflector antenna

A number of antenna types were investigated during the study, and in particular three types were looked at in detail: a conical scanning antenna, a push-broom torus reflector antenna and a push-broom twin reflector antenna consisting of two identical, shaped reflectors each providing a scan of $\pm 10^\circ$. The three types were compared and the torus push-broom reflector antenna was selected as the most promising candidate for further studies as described in the following subsections.

5.1 Reflector geometry

The push-broom antenna is a torus reflector with projected aperture D of 5 m. The torus surface is obtained by rotating a section of a parabolic arc around a rotation axis, as shown in Figure 2. The focal length f of the parabolic generator is also selected to 5 m. The angle α between the rotation axis and the parabola axis is given by the satellite height and the required incidence angle on ground. The distance p from the parabola vertex to the rotation axis is given by

$$p = f \left(2 + \tan^2 \left(\frac{\alpha}{2} \right) \right) .$$

The feed axis is selected parallel to the rotation axis, implying that all feed element axes are parallel and orthogonal to the focal plane. The feed array becomes therefore planar, simplifying the mechanical and electrical design. The reflector rim is found by intersecting the torus surface by the feed cone up to the outmost scan positions.

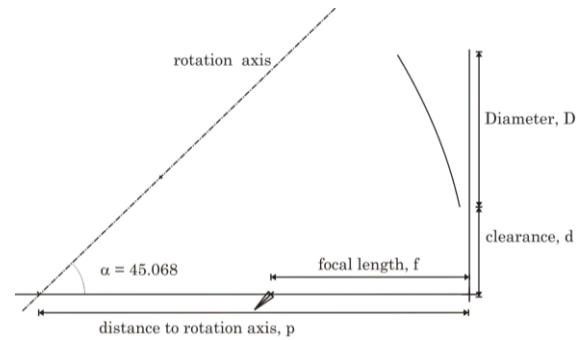


Figure 2 Push-broom torus design.

The antenna shall be able to provide a scan of $\pm 20^\circ$ corresponding to a swath width of 600 km. The final design is shown in Figure 3, where the projected reflector aperture is 5 m by 7.5 m.

The array elements are arranged in a $\rho\phi$ -grid around the rotation axis. The distance between the elements is approximately the same in the ρ -direction and in the ϕ -direction.

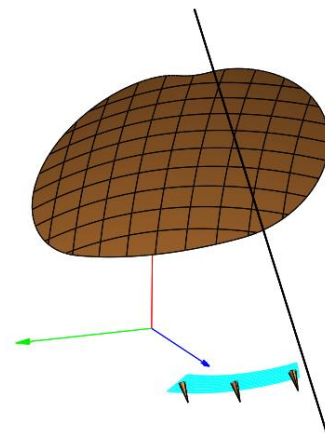


Figure 3 Torus push-broom antenna with projected aperture D of 5 m, three feeds located at 0° and $\pm 20^\circ$. The feed array is shown in green.

5.2 RF performance results

5.2.1 Central beam at Ku-band

The reflector surface is not a paraboloid and the performance is therefore expected to be most critical at the highest frequencies. In this section the central beam at Ku-band, 18.7 GHz, is presented.

The feed array has 8 elements in the ρ -direction and 21 elements in the ϕ -direction. The total number of feed array elements is therefore 168. The element excitations are determined by the optimisation approach described earlier and the result shows that 99.72% of the power from the antenna is contained inside a cone with half angle 0.5° . The synthesised excitation coefficients in amplitude are shown in Figure 4.

The far field from the feed array at 18.7 GHz is shown in Figure 5 and it is seen that the radiation outside the reflector rim is very low leading to a spill-over of only 0.05%.

The far-field pattern of the antenna is depicted in Figure 6. It is evident that this pattern is not rotational symmetric and one could therefore get the impression that the actual orientation of the coast line would be very important for the instrument performance quality. In order to check this, the central part of the beam is magnified in Figure 7 and one will see that the -30 dB contour is nearly a circle with radius 0.5° . This circle contains 99.72% of the power and the coast line can therefore be located anywhere outside this circle and its orientation is not important.

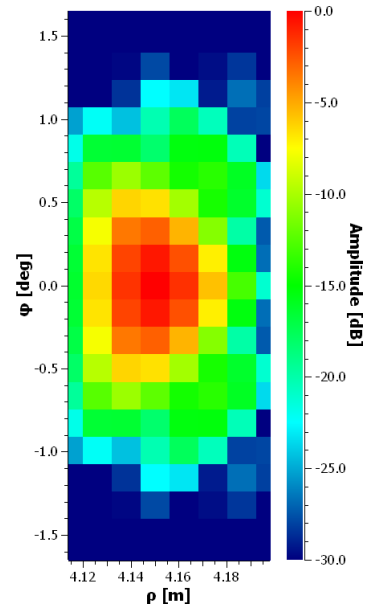


Figure 4 Excitation coefficients for the centre beam for minimum distance to coast.

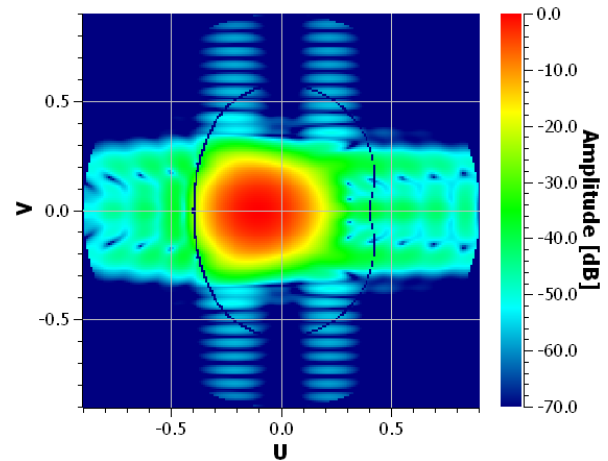


Figure 5 Far-field radiation pattern of the feed array for the centre beam.

The radiometer characteristics are shown in Table 2 and it includes not only the centre frequency but also the two band ends in order to demonstrate that the performance is almost constant across the entire band. It is noticed that the distance to coast is only 7 km.

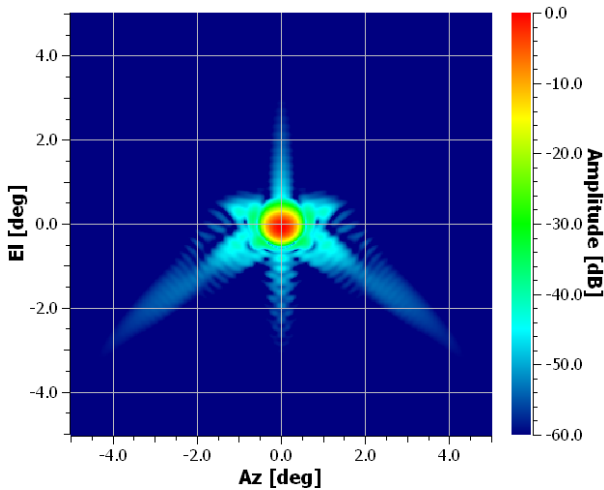


Figure 6 Image plot of the co-polar far field of the centre beam for the push-broom antenna optimised for low distance to coast.

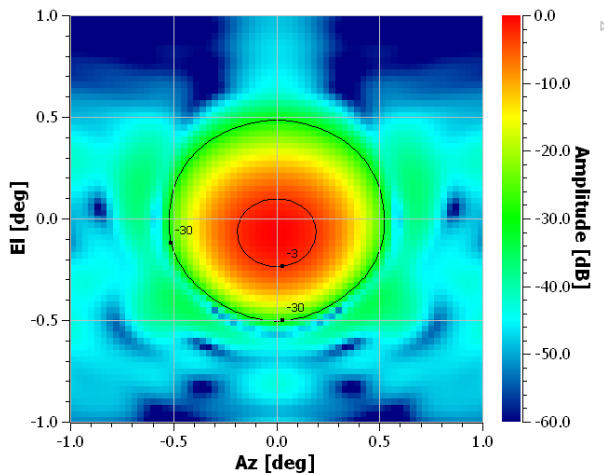


Figure 7 The central part of the pattern in Figure 6.

frequency	cr-polar power	Foot-print	Distance to coast
GHz	%	km	km
18.6	0.15	10.34	7.16
18.7	0.14	10.32	7.08
18.8	0.14	10.31	7.02

Table 2 Radiometer characteristics for the central Ku-band for the push-broom antenna optimised for low distance to coast.

5.2.2 Reduction of feed array rows along ϕ

It was demonstrated in the previous section that a feed array with 8 rows along ϕ gives a distance to coast of 7 km which is actually better than the required 15 km. We will therefore investigate if it is possible to reduce the number of feed array rows to 7 or 6 and still maintain an acceptable performance.

Figure 8 shows the optimised element excitations for 8, 7 and 6 rows. We recall that the excitations are determined such that 99.72% of the power is contained in the smallest possible cone around the beam peak. The illumination on the reflector is illustrated in Figure 9 and the resulting far-field pattern is shown in Figure 10.

The results illustrate that using a smaller number of rows generates a more elliptical illumination on the reflector and a more elliptical far-field beam. The radiometer characteristics are summarised in Table 3 and it is seen that even with only 6 rows the footprint is only slightly larger than 10 km and the distance to coast is very acceptable. It should be pointed out that for the calculation of the footprint size it is utilised that the cross section of the incident beam on the ground is elliptical.

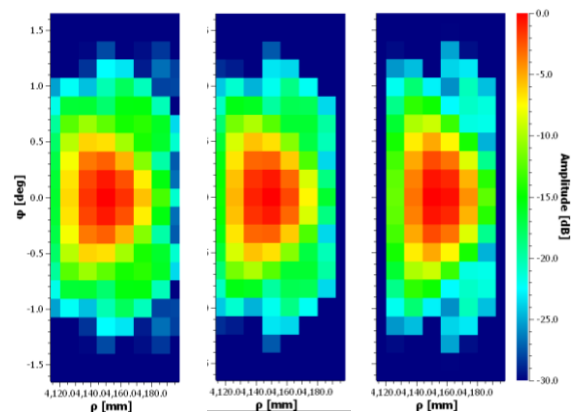


Figure 8 Optimised element excitations in amplitude using 8 (left), 7 (middle) and 6 (right) rows along ϕ .

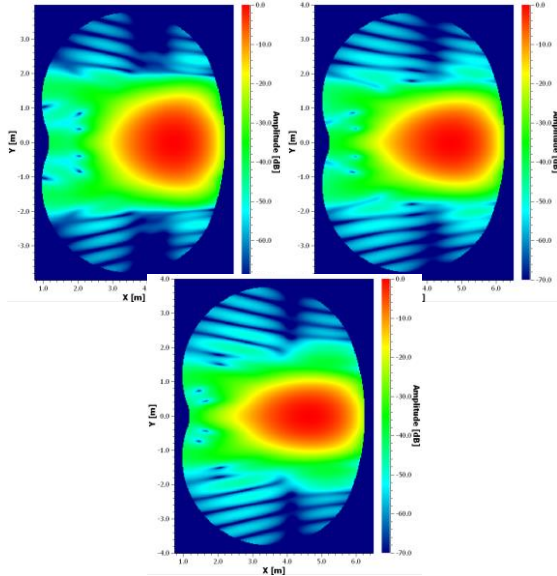


Figure 9 Reflector illumination using 8 (top left), 7 (top right) and 6 (bottom) rows along ϕ .

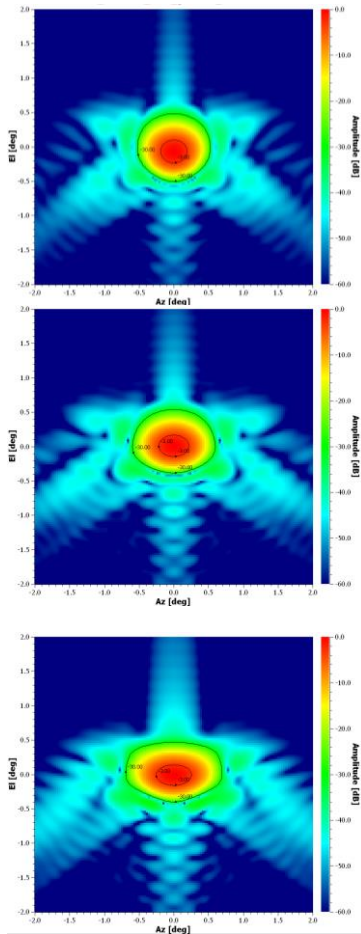


Figure 10 Far-field pattern using 8 (top), 7 (middle) and 6 (bottom) rows along ϕ .

Feed array rows along phi	Number of active elements		cr-polar power	Foot-print	Distance to coast
	x-dir.	y-dir.	%	km	km
8 rows	168	0	0.14	10.14	7.08
7 rows	147	0	0.11	10.47	7.85
6 rows	126	0	0.08	10.86	9.19

Table 3 Radiometer characteristics for the central Ku-band beam for different number of feed array rows along ϕ .

5.2.3 Total feed arrays for C-, X- and Ku-band

It was demonstrated in the previous section that acceptable performance for the centre beam at Ku-band can be achieved with a feed array containing 6 elements in the ρ -direction and 21 elements in the ϕ -direction.

We will use the same principles as for Ku-band to design the feed arrays for the centre beams for C- and X-band, still using 6x21 elements. The element excitations are determined by optimising the distance to coast and the calculated results are summarised in Table 4. It is seen that the footprint size is slightly too large at C- and Ku-band and the distance to coast exceeds slightly the required 15 km at C-band.

Frequency	cr-polar power	Foot-print	Distance to coast
	%	km	km
C-band	0.20	23.26	16.41
X-band	0.14	16.53	12.28
Ku-band	0.08	10.86	9.19

Table 4 Radiometer characteristics for the centre beam at C-, X- and Ku-band.

Having determined the feed array for the centre beam the complete feed array can be readily designed. The Ku-band feeds are located close to the focal circle of the push-broom torus and the feed arrays for C- and X-band are located on either side of the Ku-band array. The three feed arrays are shown in Figure 11. The total number of array elements is 1284, 1956 and 3156 for C-, X- and Ku-band, respectively. If 8 rows along ϕ instead of 6 were used the number of elements becomes 1616, 2480 and 4320. The latter numbers are used for the power estimates in Section 7.

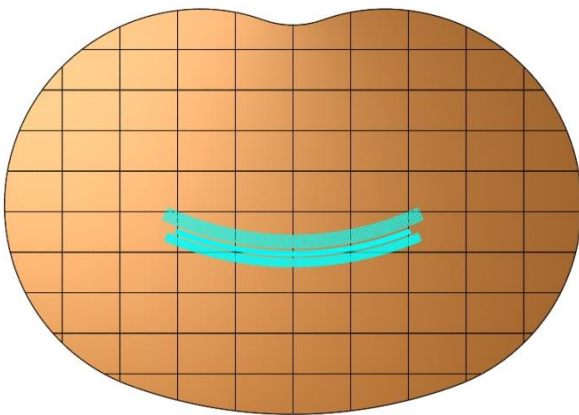


Figure 11 The feed arrays for C-, X- and Ku-band.

5.2.4 Additional performance checks

A number of different detailed investigations were carried out. The results can be summarised as follows:

Scan performance. The antenna is able to scan up to 20° to both sides without any severe scan degradations. It was found that the excitations were practically identical for all the beams but shifted in the ϕ -direction according to the actual scan direction.

Bandwidth investigations. The required bandwidth is 300, 100 and 200 MHz at C-, X- and Ku-band, respectively. The radiometer

performance was calculated at the band limits as well as the centre frequency and it was found to be almost constant over the bands.

Sensitivity to excitation inaccuracies. The feed element excitations can only be realised to certain accuracy. Two types of excitation errors were investigated. It was found that excitation errors up to 10% for each separate element and up to 3% of the largest excitation are acceptable. This is very well in line with another observation, namely that it is acceptable to discard all elements with an amplitude lower than 30 dB below the strongest excited element.

Redundancy aspects. It has been demonstrated that it is possible to re-optimize the excitation coefficients in case of a receiver failure and in this way to remedy the consequences of the failure.

Thermal distortions. A typical thermal load case for the CFRS reflector has been considered by HPS and the resulting reflector shape has been investigated by TICRA. The thermal distortions are so small that the effect on the radiometer performance is negligible.

6. Calibration and RFI mitigation

The push-broom system will use internal calibration, supported by monthly sky views using spacecraft manoeuvres. The internal calibration relies on matched loads and noise diodes. Both are established in space (SMOS and Aquarius for example). The internal calibration is augmented by active cold loads. They are as yet not established in space, but have been studied and evaluated in several ESA projects. The calibration is thus considered to be relatively standard and straight forward.

RFI will be detected and mitigated on-board. The detection is based on the following methods:

- anomalous amplitude
- Kurtosis method
- polarimetric method
- frequency domain detection

An additional and promising method, the Spectral Kurtosis, has been discussed during the study. No real experience using this method in space exists.

7. Feeding network and receiver issues

In this section the receiver resource demands – especially concerning power consumption – will be evaluated, first using existing state-of-the-art components, and second using values that can be realistically expected within a 5 years time frame.

7.1 Existing state-of-the-art components

As illustrated in Figure 12, each antenna element is assigned its own receiver and A to D converter. Hence, the total number of components in a single receiver must be multiplied onto the number of antenna elements, and a major concern is the total number of components in the system, with respect to mass, size and especially to power consumption.

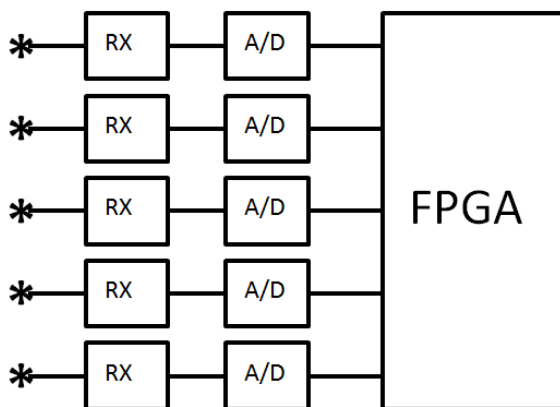


Figure 12 Dense array receiver system.

The A to D converter is the most critical component, as it is traditionally the largest and by far the most power consuming. However, over the past decade technology has developed rapidly. Most components are wideband, or similar between the three frequency bands of interest, and thus a common overview has been made for the different component types included in each receiver. The result of this shows, that a realistic power budget based on state-of-the-art components will result in a power consumption of approximately 850 mW per receiver at X-band and 1100 mW at Ku-band and C-band. The total power budget is dominated by X- and Ku-band due to the many receivers at these frequencies, and for global power budget estimates we can assume 1 W per receiver. Adding also power for beam forming network and RFI processor we end up with 1.38 W per receiver. With 8416 elements this gives a total power of 11.6 kW, which is not realistic now or in the near future.

7.2 Realistic components within a 5 years time frame

Already now A/D converters able to sub-sample signals up to X-band are available in research labs. and within very few years Ku-band is also served. The development concerning amplifiers is also impressive, especially when it comes to noise figure at high frequencies and power consumption. For global power budget estimates we can within a few years assume 49 mW per receiver, including beam forming network and RFI processor. This amounts to a total power consumption of $8416 \times 49 \text{ mW} = 412 \text{ W}$, which is certainly realistic.

8. Mechanical design of the push-broom torus antenna

The mechanical realisation of the torus reflector proposed by HPS consists of a double layer pantograph and two triangular wire nets, one in

the front and one in the back. The corners of the triangles are connected by adjustment wires, as shown in Figure 13. The front net forms the surface of the reflector. Initially it was assumed that the front net would be covered with a knitted metal mesh in order to provide the necessary RF reflection. It was realised, however, that the triangular facets would generate high and unacceptable grating lobes unless the triangles were made very small, i.e. 100 mm size. Consequently, it was proposed to construct the reflector as a doubly curved CFRS (Carbon Fibre Reinforced Silicon) surface. The triangular net is maintained to support the CFRS but the size of the triangles can be much larger, around 400 mm. It must be checked that the selected CFRS membrane material has the sufficient RF reflectivity for the requested frequency range.

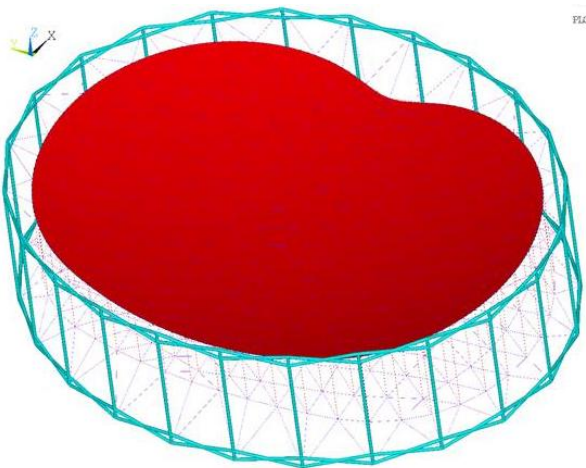


Figure 13 Mechanical realisation of the torus push-broom reflector dish.

9. Summary of results achieved

The purpose of the study was to investigate novel antenna architectures for real aperture multi-beam radiometers providing high resolution and high sensitivity for accurate ocean observation from space. The instrument was requested to accurately measure in C-, X- and Ku-band and up to only 15 km from the coast line.

Two scenarios were considered, i.e. conical and push-broom scanning. Detailed investigations were performed by the team to design a reflector antenna satisfying the requirements in both scanning schemes. A dense focal plane array was chosen, meaning that many elements take part in the formation of one beam and the same element takes part in the formation of many beams. A dedicated optimisation procedure was developed in order to find the excitation coefficients of the feed array elements and simultaneously reduce the number of the elements.

The push-broom candidate showed very high sensitivity and the big advantage of being fully stationary and was therefore chosen. The antenna underwent a detailed design, which included a study of the calibration and RFI mitigation as well as important mechanical aspects related to the light weight realization of the reflector, which has an aperture of 5 m by 7.5 m.

10. Future work

The torus push-broom antenna designed by the team provides a very high sensitivity and satisfies all radiometric requirements. However, further studies are necessary in order to account for the mutual coupling in the feed array, model the reflective surface of the light weight reflector more in detail, and design, manufacture and measure a small but representative portion of the dense feed array system, including receivers, A/D converters and FPGA.